UNIABUJA Journal of Engineering and Technology

https://ujet.uniabuja.edu.ng/

ISSN: 2714-3236 (Online); 2714-3228 (Print)

Volume 2, Issue 2, 2025; 413-427

Investigating the Effects of Acetylation Treatment on the Mechanical and Morphological Properties of Bagasse Filled low Density Polyethylene Composites

Friday A. ONUH[1], Tunde O. OGUNDANA[2], James O. ABIOYE[3], Ekundayo A. OLUMILUA[4], Kazeem A. BELLO[5], David T. GUNDU[6], Sambastine A. BAM[7]

[1,2,3,4,5]*Department of Mechanical Engineering, Federal University, Oye-Ekiti, Nigeria*
[6,7]*Department of Mechanical Engineering, Federal University of Agriculture, Makurdi, Nigeria*

[1]*friday.onuh@fuoye.edu.ng*, [2]*tunde.ogundana@fuoye.edu.ng*, [3]*james.abioye@fuoye.edu.ng* , [4]*adebisi.olumilua@fuoye.edu.ng*
[5]*kazeem.bello@fuoye.edu.ng*, [6]*Terfa.gundu16@gmail.com.*, [7]*sebastinebam240@gmail.com*

Abstract

This study investigates the effect of acetylation treatments on the mechanical and thermal properties of bagasse filler low density polyethylene composites (LDPEC). The treated bagasse filler LDPEC exhibited improved flexural strength, tensile strength, impact strength, and water absorption resistance compared to non-treated LDPEC. Fourier Transform Infrared (FTIR) spectroscopy and Scanning Electron Microscopy (SEM) analysis revealed enhanced interfacial bonding and filler dispersion in the treated LDPEC. Dynamic Mechanical Analysis (DMA) showed improved storage modulus and loss modulus values for treated PEC. The results demonstrate that acetylation treatment of bagasse filler can significantly enhance the mechanical and thermal properties of LDPEC such as in flexural strength 4.1Mpa to 6.9Mpa for 10% filler loading 5.7Mpa to 7.3Mpa for 20% filler loading and 6.9Mpa to 9.4Mpa , and tensile strength (2.5 to 2.8, 3.1 to 4.6, 4.7 to 6.9)Mpa for NTBFPEC to ACTBFPEC making them suitable for various engineering applications.

Keywords: *Bagasse filler, polyethylene composites, chemical treatment, mechanical properties, thermal properties.*

1.0 Introduction

Composites combine properties from multiple materials to create engineered solutions with enhanced performance. Typically, they consist of a matrix phase, which provides structure, and a dispersed phase, which reinforces strength (Miracle and Donaldson, 2003). Composites are advanced materials engineered by combining two or more distinct constituents to achieve superior properties that are unattainable by the individual components alone. Typically, these materials are composed of a matrix phase—such as a polymer, metal, or ceramic—that serves as the continuous medium providing shape and environmental resistance, and a dispersed or reinforcement phase—often fibers or particulates—that imparts mechanical strength, stiffness, and improved functional performance (Miracle & Donaldson, 2001).The synergy between matrix and reinforcement allows composites to be tailored for specific structural or functional applications, offering benefits such as high strength-to-weight ratios, corrosion resistance, and fatigue durability. Recent advancements in composite technology have focused on the development of multifunctional materials, nanocomposites, and sustainable bio-based composites to meet the evolving demands of aerospace, automotive, civil infrastructure, and renewable energy sectors (Jawaid *et al.*, 2020; Chatterjee, 2021; Nair & Laurencin, 2020). Moreover, innovations in manufacturing techniques such as automated fiber placement, 3D printing, and resin infusion processes have enhanced the design flexibility and cost-effectiveness of composite structures (Campbell, 2021). By integrating materials science, mechanical design, and processing technologies, composite materials continue to play a vital role in the development of high-performance, lightweight, and durable engineered solutions across diverse industries.

In recent years, composites have become integral to engineering applications, increasingly replacing metals and ceramics due to their cost-effectiveness, availability, and customizable properties. However, environmental concerns have increase interest in biodegradable, sustainable alternatives derived from renewable resources (Nishino, 2004). Natural fibre-reinforced polymer (FRP) composites are gaining prominence due to their low density, flexibility, cost-effectiveness, and ease of processing (Valadez *et al.*, 1999). They are widely used in industries such as construction, furniture, and automotive manufacturing (Zampaloni *et al.*, 2007).

Among natural fibres, bagasse—a by-product of sugarcane processing—presents a significant opportunity for composite reinforcement. Although commonly used as fuel, global production exceeds demand, leaving substantial quantities unutilised (Rasul *et al.*, 1999; Mulinari *et al.*, 2009). Bagasse-reinforced

Received: 15-03-2025 / Accepted: 19-05-2025 / Published: 29-09-2025

https://doi.org/10.70118/ujet.2025.0202.37

composites have demonstrated benefits such as recyclability, biodegradability, high specific strength, and environmental sustainability (Satyanarayana *et al*., 2009; Inuwa, 2013; Lu Na *et al*., 2012).
The push for sustainable materials has also driven interest in biodegradable composites, particularly in rubber compounding, where short fibres improve mechanical properties and processing efficiency (Sain et al., 2005; Gonzalez and Ansell, 2009). However, natural fibres moisture absorption is limiting their compatibility with polymer matrices due to moisture sensitivity and poor adhesion (Beroti *et al*., 2009). Surface modification, through physical or chemical treatment, is essential to improve fibre-matrix bonding by removing impurities that hinder adhesion (Thamae *et al*., 2007; Dittenber and Gangarao, 2012; Bledzki *et al*., 1996). This process increases surface roughness, enhancing mechanical interlocking and overall composite performance (Wu *et al*., 2000; Sulawan *et al*., 2012).

Despite an annual global bagasse production of approximately 54 million dry tonnes (Mulinari *et al*., 2009), significant quantities remain unused. Studies show that incorporating bagasse as a filler in polyethylene composites enhances rigidity, hardness, tensile strength, and bending strength (Agunsoye and Aigbodion, 2013). However, the absence of fibre chemical treatment in such studies highlights the need for improved fibre-matrix adhesion to optimise composite performance. Natural fibres offer advantages such as low cost, availability, and environmental sustainability, yet their hydrophilic nature limits their full potential in polymer composites. Research into chemical and physical fibre treatments continues to address this challenge, with certain treatments proving more effective for specific fibres (Haque *et al*., 2010). This study will explore the selection of bagasse fibre and polymer for composite production, to assess the impact of acetylation treatments on the fibre-matrix interface and the resulting composite properties.

2.0 Materials and Method

2.1 Materials

2.1.1 Material used for the study

The material for the study is presented in Table 1

Table 1: Material for study and its source

S/N	Material for Study	Location
1	Sugar cane fibres	Lokoja
2	Low density Polyethylene	Onitsha
4	Polyvinyl Acohol (PVA)	Makurdi
5	Catalystic perchoric acid	Makurdi
6	Mould release spray	Makurdi
8	Absorbent Paper	Makurdi
10	Acetic anhydride	Makurdi
11	Ethyl alcohol	Makurdi
12	Acetic acid	Makurdi

2.1.2 The Equipment used for the study

The equipment used for the study is represented in Table 2

Table 2: Equipment and Their Models

S/N	Equipment	Model	Location
1	Universal Material Testing Machine	Enerpac cat.nr.261	A.B.U Zaria
2	Monsanto Tensometer	Type "W" S/No. 9875	A.B.U Zaria
3	Cary630 FTIR	Agilent Technology	A.B.U Zaria
4	Stop Watch	Made In Germany	Makurdi
6	Mould	Locally Made	Makurdi
7	Scanning Electron Microscope	Phenom Prox. No. MVEO 16477830	A.B.U Zaria
8	Charpy Impact testing machine	Avery Denison cat.nr.412	A.B.U Zaria
9	Dynamic Mechanical Analyser	Netzch no. 242E	A.B.U Zaria
10	Digital Electronic Weighing Balance	Golden Mettler USA	U A M Makurdi

2.2 Method

2.2.1 Material preparation

The sugar cane fibres (*Bagasse*) were collected from New market also known as the international market Lokoja, Kogi state. These fibres was soaked in water for 48 hours to enable easy separation of dirt that might stick to the bagasse then it was washed with water several times to remove dirt, residual sugar and organic matter from the fibers. The fibres was sun dried to remove water and moisture content. These fibre were grounded into powder form and sieve analyses was used to achieve 10µm and the filler was stored in air tight container for preparation of test sample for further experimentation.

2.2.2 Acetylation treatment of bagasse filler

The test samples were soaked in 5% concentration of acetylene solution which consist of acetic acid with acetic anhydrides acting as the catalyst for 5hours, the fillers was removed from the solution then wash with distilled water to ensure that the filler were effectively clean. After the washing process the filler were dried at room temperature for 24hours follow by oven drying at 100^0C for 20 minutes to remove all the moisture. The fillers were stored and designated as Aceetylated treated bagasse filler (ACTBF) (oladele et al 2020;, Liu *et al* 2023;, Jimenes *et al* 2020;, silviana *et al* 2018)

2.2.3 Preparations of composite sheets

The hand lay-up method with a wooden mould of dimension 400 × 400 × 10 mm was used for casting composite sheets. The sample composites were manufactured with 10, 20, 30, 40 and 50% weight fraction of both non treated and chemically treated bagasse filler. To produce 10 wt% of non-treated bagasse filler PEC (NTBF),10 wt% of non-treated bagasse filler was added to 90 wt% of melted low density polyethylene and were mixed together applying gentle stirring to minimize air entrapment. For quick and easy removal of composite sheets, a mould releasing agent was applied on the inner surface of the mould. Then carefully, the mixture of melted low density polyethylene and bagasse filler was poured into the mould and care was taken to avoid formation of air bubbles. Pressure was applied from the top of the mould and the mould was allowed to cure at room temperature after which, the composite sheet was taken out of the mould. These procedures was adopted for preparation of 10, 20, 30, 40 and 50 % weight fraction of chemically treated and non-treated bagasse filler weight fractions for the production of all the composites samples

2.2.4 Mechanical Tests

2.2.4.1 Flexural strength test

The flexural test was carried out using a 100 kN capacity Enerpac Universal materials Testing Machine in accordance with ASTM D790 using the 3-point bending fixture utilizing centre loading on a simple supported beam with bar of rectangular cross section resting on two supports and were loaded by means of a loading nose midway between the supports. The dimension of the sample was 100 × 30 × 7 mm. The flexural test was carried out on two samples, and the average of the test values was taken.

The flexural inter laminar shear strength (ILSS) of the composite which is the maximum shear stress that a material can withstand before it ruptures, was determined using the equation 1

$$6f = \frac{3pl}{2bt^2} \qquad (1)$$

where σ_f is the ILSS, ***p*** is the load,l is the span length ***b*** is the width and t is the thickness of thespecimen under test.

The procedures was adopted for all composite specimens and the flexural modulus (E) were determined using equation 2.

$$E = \frac{pl^3}{4bt^3Y} \qquad (2)$$

Where *Y*= deflection, l =span length, *p*= load, **b** = width, *t* = thickness.

2.2.4.2 Tensile strength test

Tensile strength test was carried out in accordance with ASTM D638 procedures using a Monsanto tensometer (type "w").The sample dimension was 100 ×30 × 5 mm, gauge length of 40 mm, the samples were clamped at either end on the machine and pulled apart until failure occurred .The tensile test was done on two samples and the average of the values was taken

The maximum tensile stress was determined using equation 3.

$$6t = \frac{F}{A} \qquad (3)$$

Where F= applied load, and A= cross sectional area of the sample.

The tensile strains were determined using equation 4.

$$E = \frac{l_2 - l_1}{l_1} \qquad (4)$$

Where L_1= gauge length and L_2= length after test.

2.2.4.3 Impact strength test

The impact test of the samples with dimensions 100×30×10 mm was done using the Avery Denison Charpy Impact Testing Machine with capacity 15J in accordance with ASTM standard D-256.. The samples were clamped into the impact machine and were subjected to impact energy of 15 Joules with a pendulum of

Received: 15-03-2025 / Accepted: 19-05-2025 / Published: 29-09-2025

https://doi.org/10.70118/ujet.2025.0202.37

25kg striking the sample at the rate of 3.21m/s. The impact test was done on three samples and the average of the values of the impact energy was recorded, from which the impact strength was calculated using equation 5.

$$I = \frac{K}{A}\left(\frac{\text{kJ}}{m^2}\right) \quad (5)$$

where K = Impact Energy (kJ), A = Cross-sectional area = width (m) × thickness (m)

2.2.4.4 Water absorption test

The water absorption test was performed on the composite material in accordance with ASTM standard D570, The bagasse filler reinforced polyethylene composite were oven dried to ensure removal of moisture content and was weighed to constant weight (M_A). The composites were immersed completely in distilled water for 72hours at room temperature after which the composite samples was removed from water, the surfaces dried with absorbent paper and weighed immediately to determine the weight (M_B) after immersion of bagasse filler reinforced polyethylene composites. The differences in weight were used to determine the percentage of water absorption of the samples using equation 6.

$$\text{Percentage of water absorption} = \frac{M_{B-}M_A}{M_A} \times 100 \quad (6)$$

Where M_A = mass of sample before soaking, M_B= mass of sample after soaking in water.

2.2.4.5 Surface Morphology Test

Surface morphology properties were examined using the Scanning Electron Microscope Phenom Prox. The samples were cleaned properly and to ensure all unwanted particles sticking to the surface was removed, sand paper was used to rub the surface of the composite and the samples was air-dried. The composite specimens was examined directly using the Phenom Scanning Electron Microscope Model: To enhance the conductivity of the samples, a thin film of platinum was vacuum-evaporated onto samples before the photomicrographs were taken.

2.2.4.6 The Fourier Transform Infrared Spectroscopy (FTIR)

The bagasse filler reinforced polyethylene composite was scraped from the surface to obtain some particles, these particles was mixed with potassium bromide (Kbr) powder and it is ground to reduce the particle size, until crystallities could no longer be seen and until it became pasty and sticky and a pellet is formed. the pellet was put on IR plate and the spectra were taken.

2.2.4.7 Dynamics Mechanical Analysis (DMA)

The Dynamic Mechanical Analysis (DMA) was carried out in accordance with ASTM D7028. using Netzch Dynamic Mechanical Analyser (DMA) Model no. 242E with an inbuilt data acquisition software. The Sample with dimensions 60 × 12 × 5mm were placed in the furnace manually on a holder using a clamp. The clamp is made up of two parts, the upper part and the lower part, which is movable, the clamp was then closed by pressing the clamp button. Upon loading the sample, the temperature was raised to 30 °C and allowed to stabilize. The chamber was heated at a rate of 10 °C per minute until 110 °C. The analysis was performed in dual cantilever mode with oscillation amplitude of 60 µm, at frequencies of 1 Hz, 2 Hz and 5 Hz. This system has in-built software which analyses the experimental data for the storage modulus, loss modulus and damping factor (tan d) and record them as functions of temperature.

2.2.5 Experimentation (design)

2.2.5.1 Experimentation/design of the chemical solution

The design and detailed composition of chemical solution are shown in Table 3. Five percent (5%) concentration of solution were employed for the chemical treatments.

Table 3: Optimized Chemical Formulation for Acetylation Treatment of Bagasse Filler

S/N	Solution name	Solution composition
1	Acetylating solution	950cm^3 of water + 5g of acetic acid + 2g of acid anhydrides

2.8.2 Experimentation /Design of composite

Table 4: Design of Non Treated Bagasse Filler (NTBF) Composite

S/N	Sample	Composition (by wt. %)
1	10 wt. % NTBF LDPEC	90 wt. % of low density polyethylene + 10 wt. % of non-treated Bagasse filler
2	20 wt. % NTBF LDPEC	80 wt. % of low density polyethylene + 20 wt. % of non-treated Bagasse filler

Received: 15-03-2025 / Accepted: 19-05-2025 / Published: 29-09-2025

https://doi.org/10.70118/ujet.2025.0202.37

S/N	Sample	Composition (by wt. %)
3	30 wt. % NTBF LDPEC	70 wt. % of low density polyethylene + 30 wt. % of non-treated Bagasse filler
4	40 wt. % NTBF LDPEC	60 wt. % of low density polyethylene + 40 wt. % of Non-treated Bagasse filler
5	50 wt. % NTBF LDPEC	50 wt. % of low density polyethylene + 50 wt. % of Non-treated Bagasse filler

Table 5: Design of Acetylated Treated Bagasse Filler (ACTBF) Composite

S/N	Sample	Composition (by wt. %)
1	10 wt. % ACTBF LDPEC	90 wt. % of low density polyethylene + 10 wt. % of Acetylated treated Bagasse filler
2	20 wt. % ACTBF LDPEC	80 wt. % of low density polyethylene + 20 wt. % of Acetylated treated Bagasse filler
3	30 wt. % ACTBF LDPEC	70 wt. % of low density polyethylene + 30 wt. % of Acetylated treated Bagasse filler
4	40 wt. % ACTBF LDPEC	60 wt. % of low density polyethylene + 40 wt. % of Acetylated treated Bagasse filler
5	50 wt. % ACTBF LDPEC	50 wt. % of low density polyethylene + 50 wt. % of Acetylated treated Bagasse filler

3.0 Results and Discussion

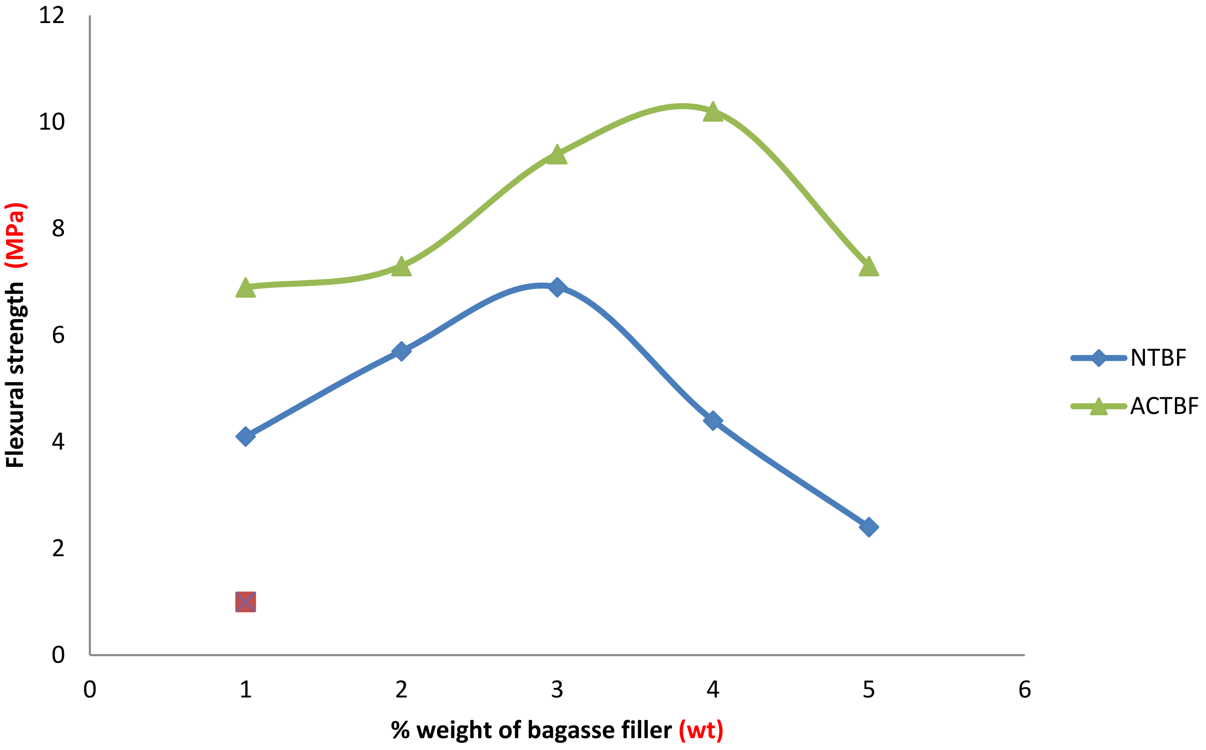

Figure 1: Variation of flexural strength with composition of bagasse filler in LDPEC

3.1 Flexural Strength

The treated filler's ACTBF LDPEC exhibited higher flexural strength than the non-treated bagasse filler (NTBF) LDPEC. Chemical treatment enhanced surface roughness, resulting in improved mechanical interlocking and increased cellulose exposure. This was confirmed by FTIR spectroscopy, which showed removal of hydrogen bonds, O-H groups, lignin, wax, and oil from the filler's surface.

The ACTBF LDPEC achieved the highest flexural strength value of 10.2 MPa at 40 wt% bagasse filler reinforcement. This was attributed to the introduction of acetyl groups, which substituted hydroxyl groups, enhancing fibre-matrix adhesion (Sreekala, 2003; Hill et al., 1998).

Received: 15-03-2025 / Accepted: 19-05-2025 / Published: 29-09-2025
https://doi.org/10.70118/ujet.2025.0202.37

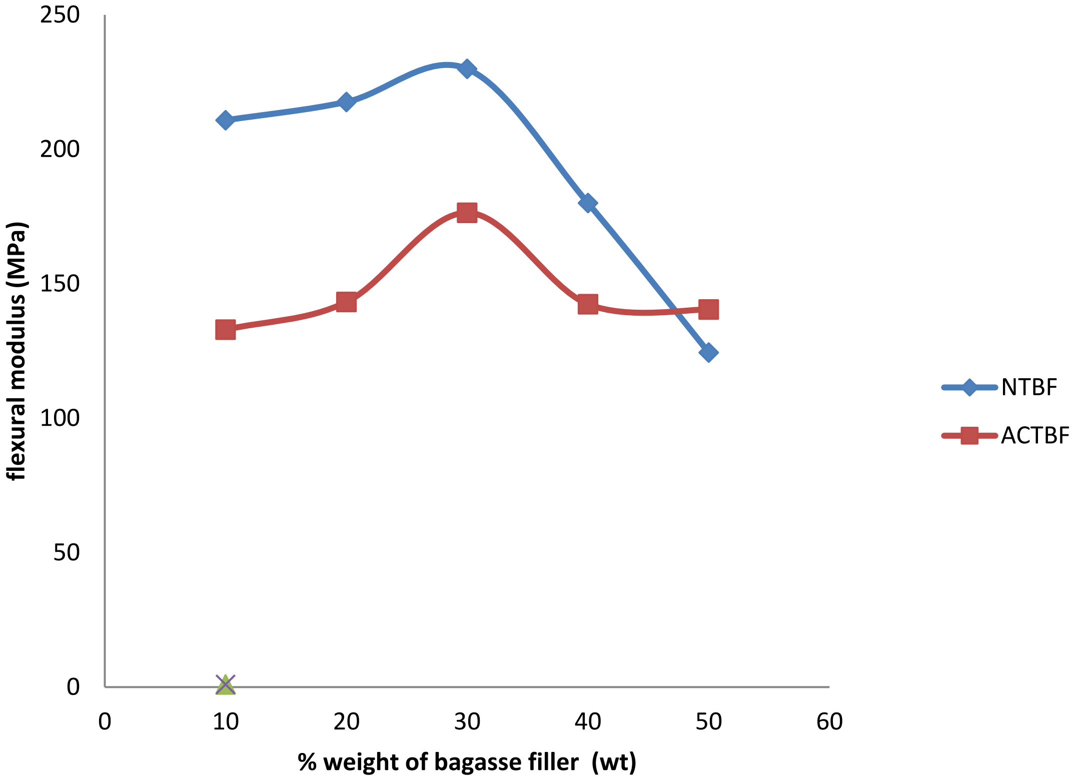

Figure 2: Variation of flexural modulus with composition of bagasse filler in LDPEC

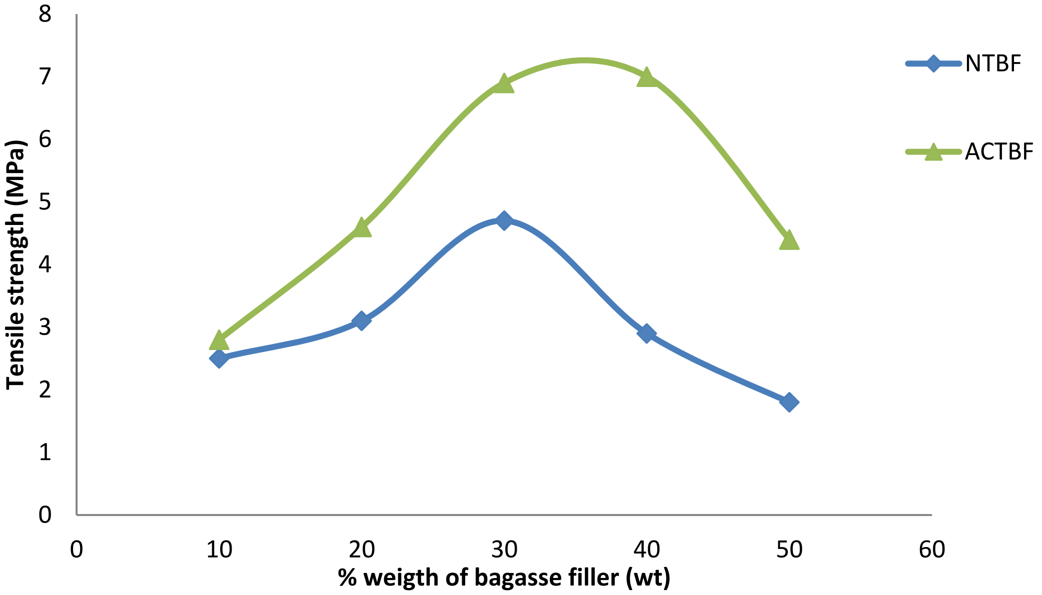

Figure 3: Variation of tensile strength with composition of bagasse filler in LDPEC

3.2 Tensile Strength

The tensile strength of ACTBF LDPEC was found to be higher than that of NTBF PEC, as shown in Figure 3. This improvement is consistent with previous studies (Torres et al., 2005; Tserki et al., 2000) and is attributed to the chemical treatment of the bagasse filler, as evidenced by FTIR spectroscopy. For ACTBF LDPEC, the tensile strength increased with increasing filler composition from 10 wt% to 40 wt%, 2.5, to 2.8Mpa, 3.1 to 4.6Mpa, 4.7 to 6.9Mpa and 2.9 – 7mpa respectively from the NTBF PEC due to improved adhesion between the filler and matrix resulting from acetylation (Nair et al., 2001; Sreekala, 2003). The treated filler LDPEC exhibited higher tensile strength than the non-treated filler PEC, as shown in Figure 3, due to enhanced filler dispersion, bond creation between polyethylene and bagasse filler, and improved wettability (Xu et al., 2001; Colon et al., 2003). This improvement aligns with recent findings (Rahman et al ., 2022; Zhang et al 2020)

Received: 15-03-2025 / Accepted: 19-05-2025 / Published: 29-09-2025

https://doi.org/10.70118/ujet.2025.0202.37

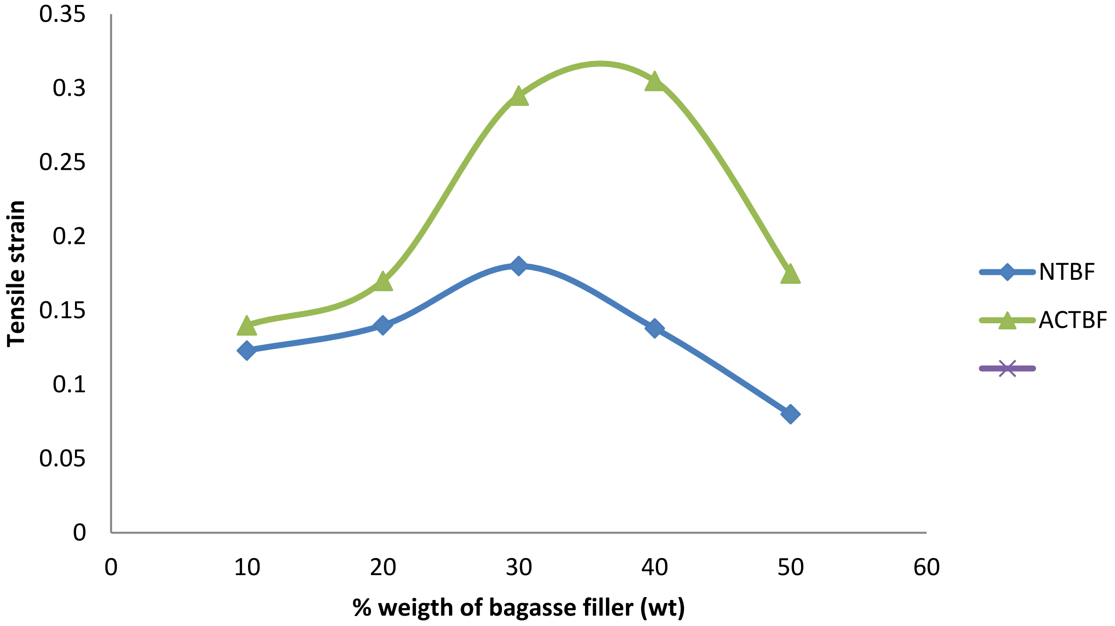

Figure 4: Variation of tensile strain with composition of bagasse filler in LDPEC

3.3 Tensile Strain

Figure 4 shows that the tensile strain of chemically treated bagasse filler LDPEC (ACTBF) is greater than that of non-treated bagasse filler LDPEC (NTBF). This improvement is attributed to enhanced interfacial bonding, wettability, and mechanical interlocking between the filler and matrix (Nair et al., 2007).

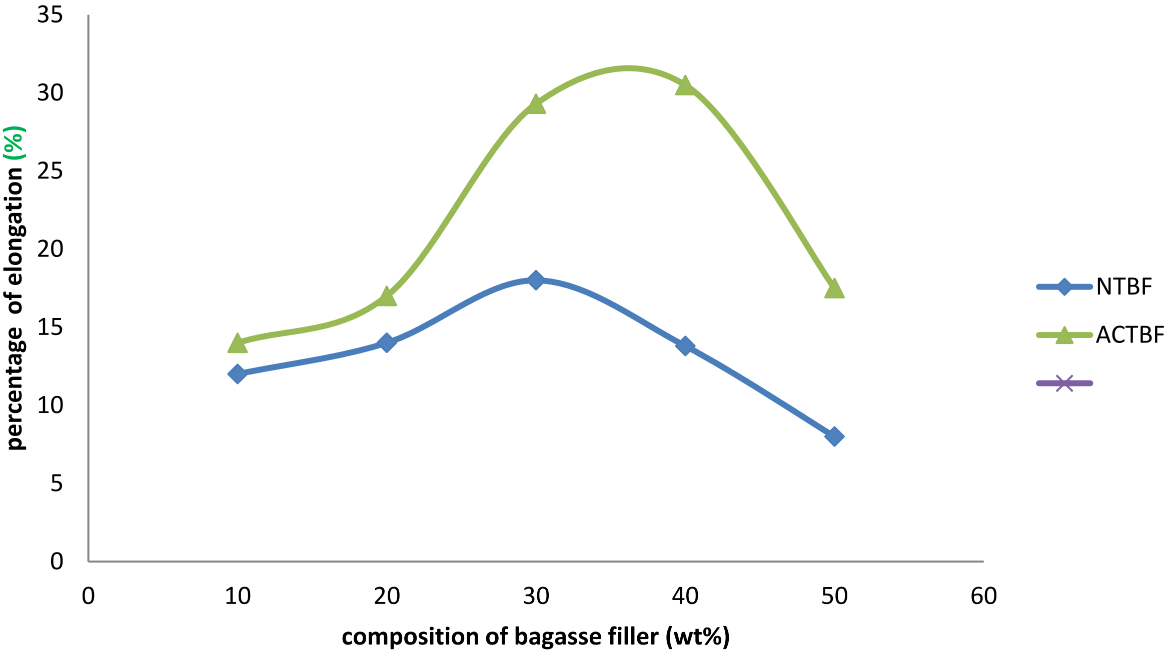

Figure 5: Variation of percentage elongation with composition of bagasse filler in LDPEC

3.4 Percentage Elongation

Figure 5 indicates that the percentage elongation of treated bagasse filler ACTBF LDPEC is higher than that of NTBF LDPEC. This improvement is due to good dispersion of the filler in the polyethylene matrix and strong interfacial bonding between the filler and polymer.

Received: 15-03-2025 / Accepted: 19-05-2025 / Published: 29-09-2025

https://doi.org/10.70118/ujet.2025.0202.37

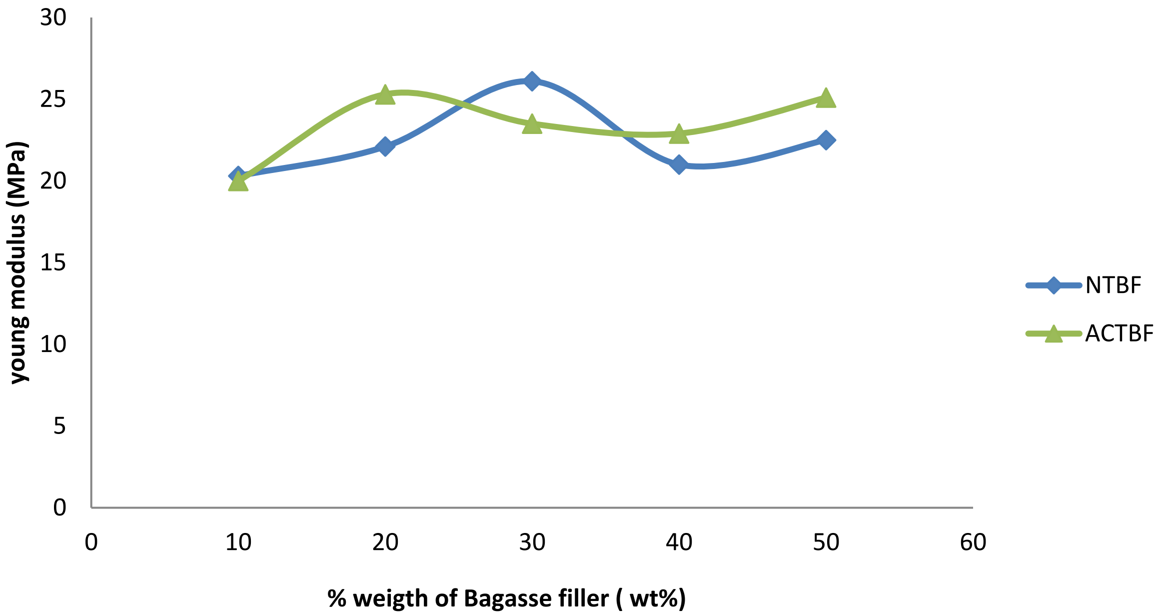

Figure 6:Variation of Young Modulus with composition of bagasse filler in LDPEC

3.5 Young's Modulus

Figure 6 shows that the Young's modulus of ACTBF LDPEC is higher than that of NTBF LDPEC at 20 Wt% bagasse filler loading. This improvement is attributed to the chemical treatment, which enhances filler dispersion, interfacial bonding strength, and introduces more reaction sites (Arrakhiz et al., 2013).

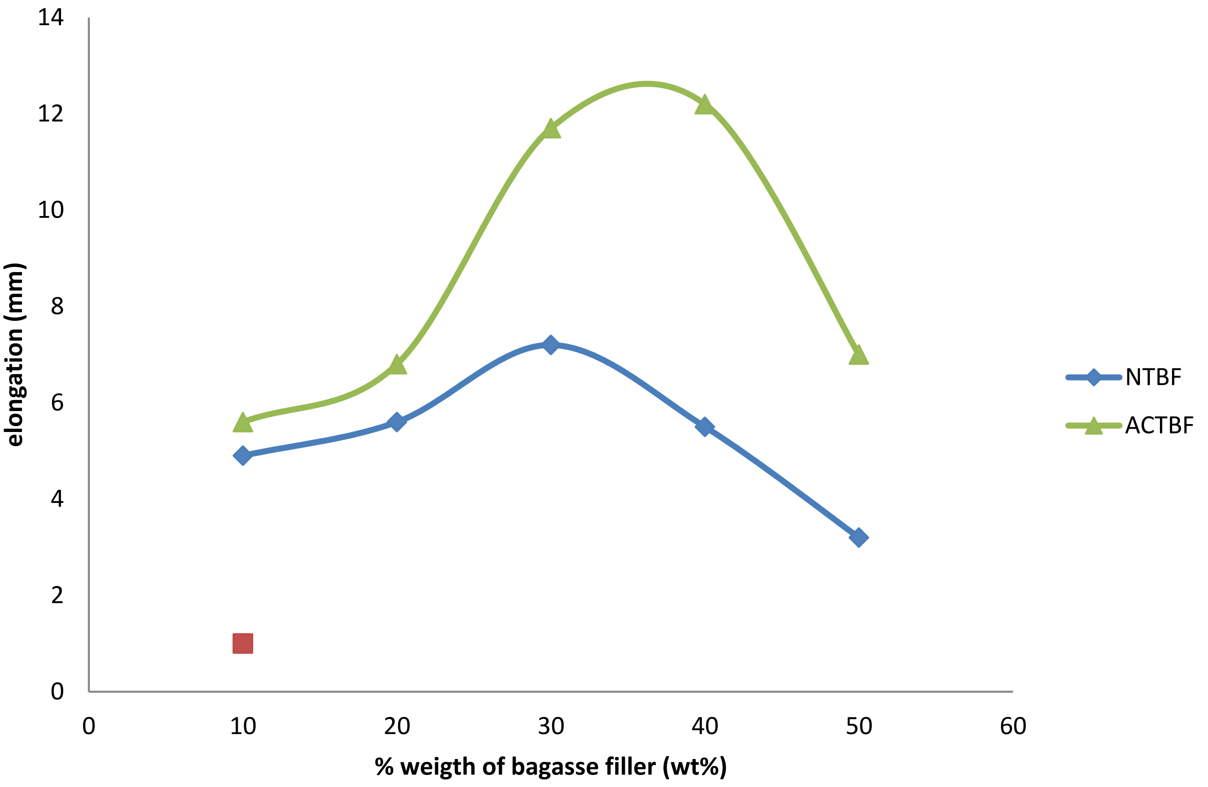

Figure 7: Variation of elongation with composition of bagasse filler in LDPEC

3.6 Longation

The elongation of treated bagasse filler LDPEC is higher than that of non-treated bagasse. This improvement is attributed to the creation of an interface area that permits better mechanical interlocking, enhancing the bond strength between the filler and polyethylene matrix. DMA analysis shows that treated bagasse filler LDPEC is more elastic than non-treated bagasse LDPEC, as evident from the loss factor in Figures 27-30.

Received: 15-03-2025 / Accepted: 19-05-2025 / Published: 29-09-2025

https://doi.org/10.70118/ujet.2025.0202.37

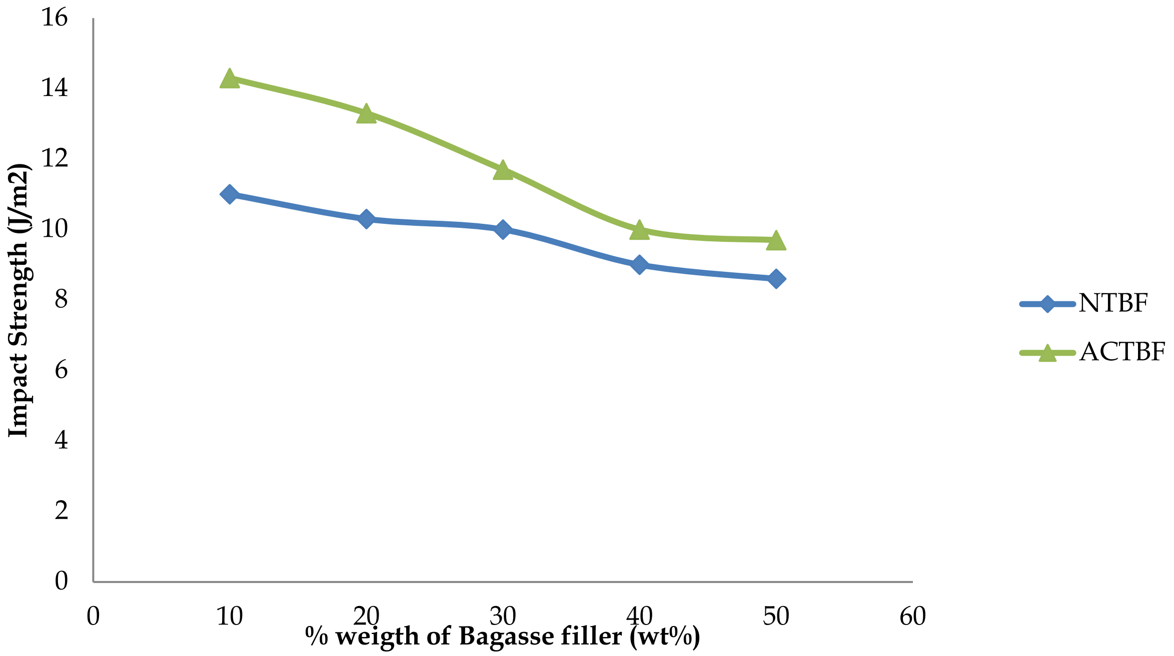

Figure 8: Variation of impact strength with composition of bagasse filler in LDPEC

3.7 Impact Strength

Figure 8 shows that the impact strength of treated bagasse filler composite is higher than that of non-treated bagasse filler composite (Islam et al., 2011). This improvement is attributed to uniform particle distribution and enhanced adhesion between the matrix and filler due to chemical treatment. However, the impact energy decreases with increasing bagasse filler loading, as the filler reduces the matrix's ability to absorb energy (Wang et al., 2010; Agunsoye and Aigbodun, 2013).

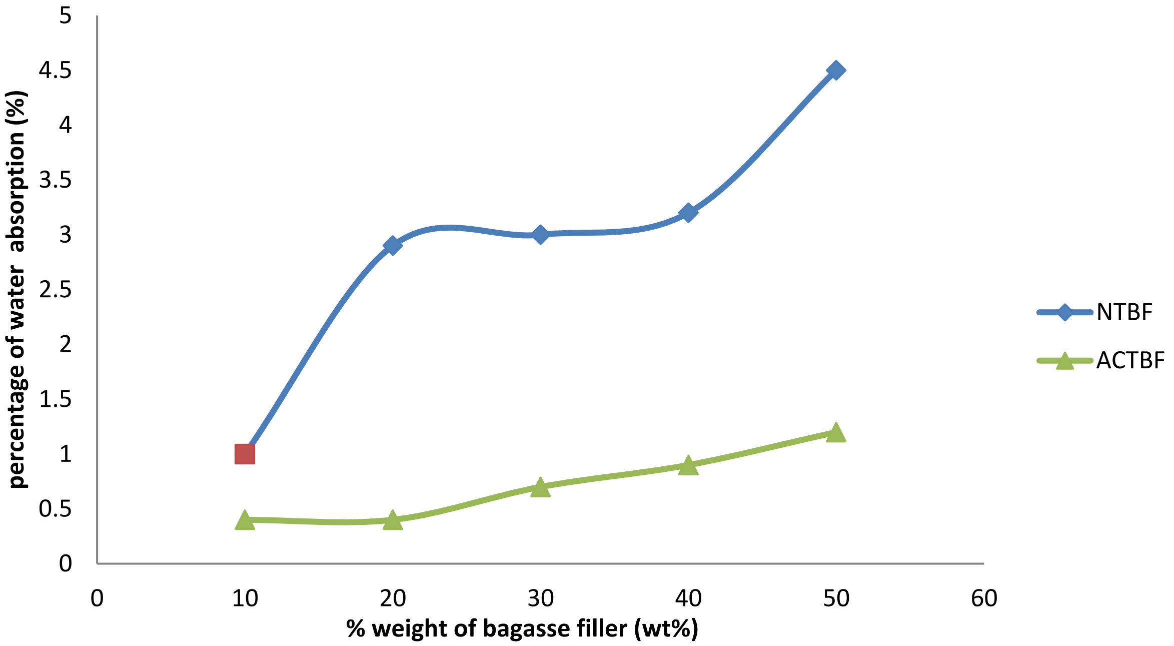

Figure 9: Variation of water absorption rate with composition of bagasse filler in LDPEC

3.8 Water Absorption Rate

The treated bagasse filler LDPEC exhibited improved water absorption resistance compared to the non-treated LDPEC. However, water absorption increased with bagasse content in the polymer matrix. Chemical treatment significantly reduced water absorption, with acetylation decreasing it by over 50% (Luz et al., 2008). This is attributed to the removal of hydroxyl groups and introduction of new functional groups, as evident in the FTIR spectrum of ACTBF LDPEC.

Received: 15-03-2025 / Accepted: 19-05-2025 / Published: 29-09-2025

https://doi.org/10.70118/ujet.2025.0202.37

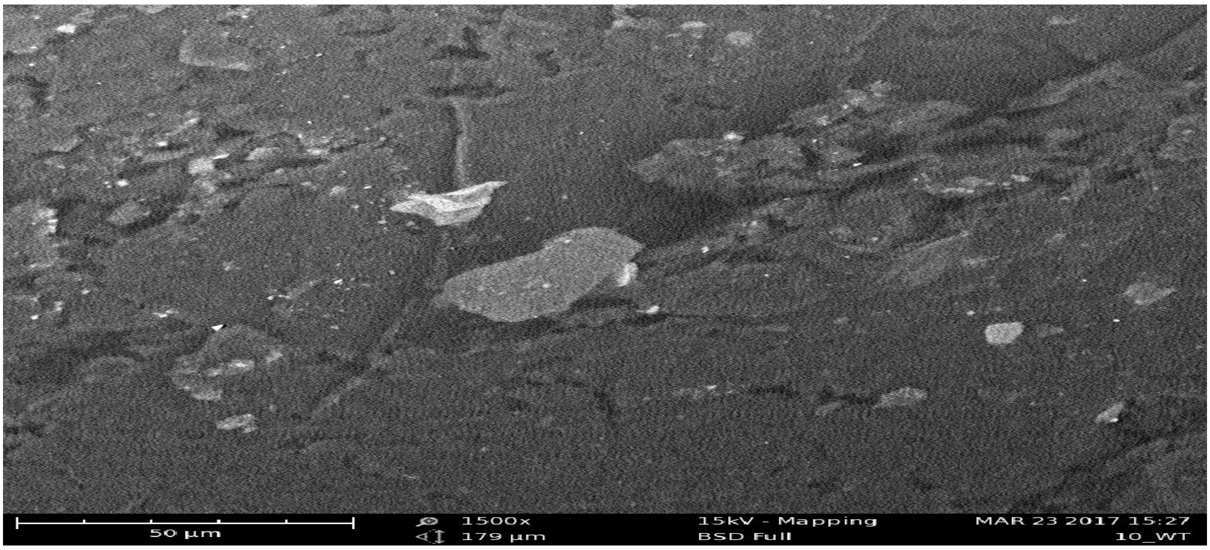

Figure 10: SEM Photography of non treated bagasse reinforced LDPEC

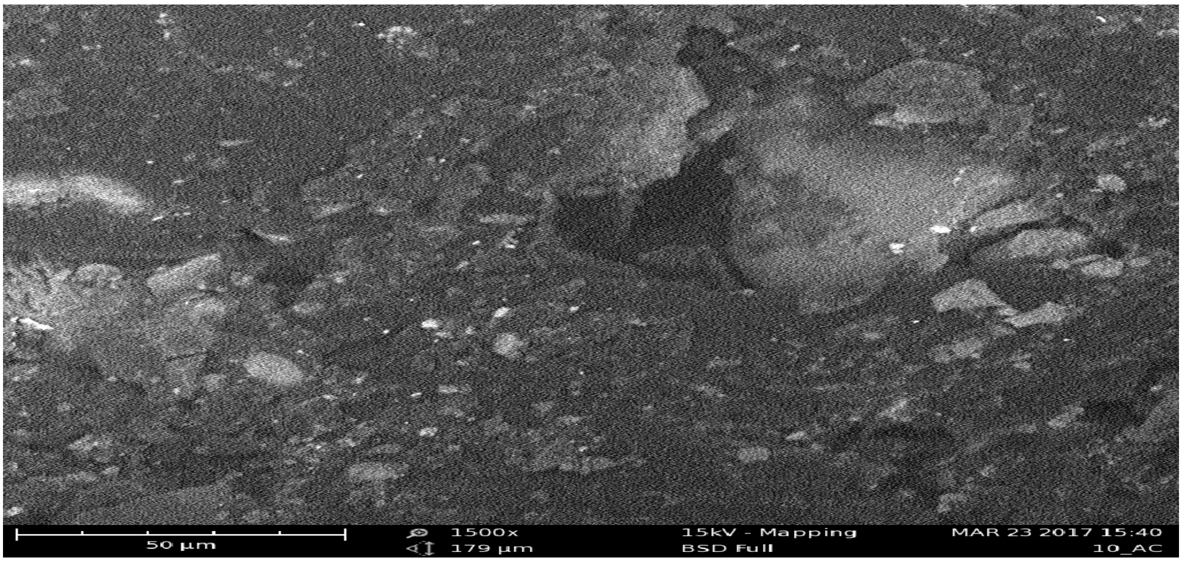

Figure 11: SEM photography of acetylated treated LDPEC

3.9 Surface Morphology Analysis

SEM analysis revealed distinct morphological differences between treated and non-treated LDPEC. The treated bagasse filler LDPEC (ACTBF) exhibited a rougher surface than the non-treated LDPEC (NTBF), indicating improved adhesion between the bagasse filler and polyethylene matrix. The surface morphology also showed proper mixing of the bagasse filler with the polyethylene matrix, establishing a strong interface.

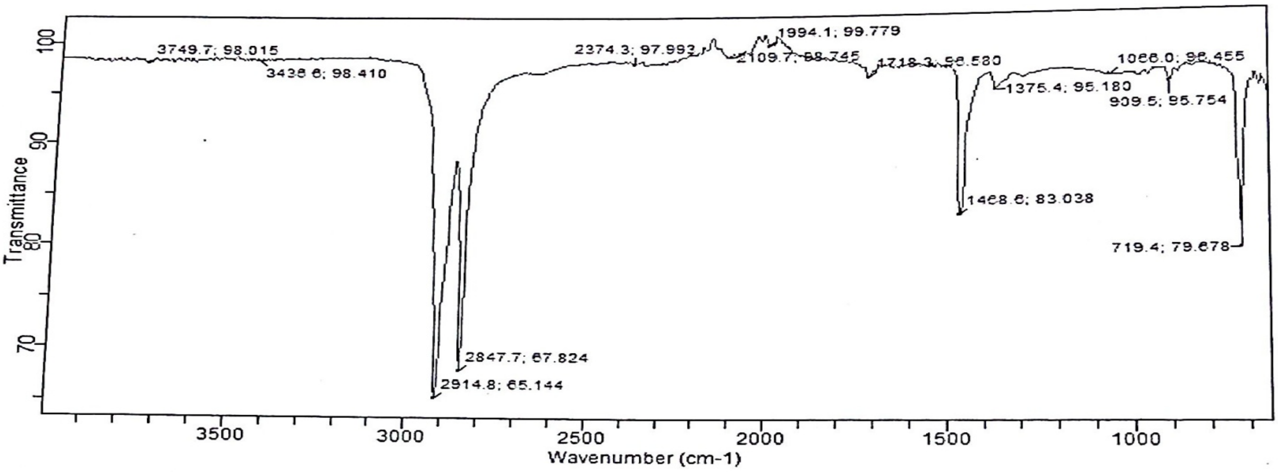

Figure 12: FTIR Spectroscopy of non treated bagasse reinforced LDPEC

Received: 15-03-2025 / Accepted: 19-05-2025 / Published: 29-09-2025

https://doi.org/10.70118/ujet.2025.0202.37

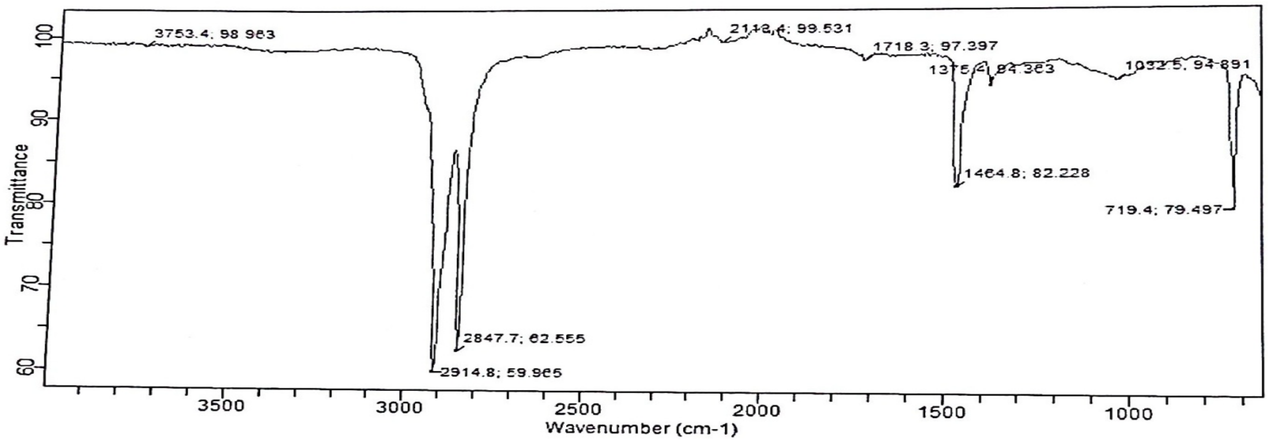

Figure 13: FTIR Spectroscopy of acetylated bagasse reinforced LDPEC

3.10 Fourier Transform Infrared (FTIR) Spectroscopy Analysis of LDPEC

FTIR spectroscopy provided quantitative and qualitative information on the chemical composition and bonding of LDPEC. The spectra revealed distinct differences between treated and non-treated LDPEC.The NTBF LDPEC spectrum (Figure 12) showed characteristic absorption bands for cellulose, including OH-stretching vibrations (3749.7-798.015 cm-1 and 3436.6-698.410 cm-1). The bands at 2914.8-65.144 cm-1 and 2847.7-67.872 cm-1 represented CH2 asymmetric and symmetric stretching, respectively. The ACTBF LDPEC spectrum (Figure 13) showed significant changes, including reduced OH absorption (3753.4-98.963 cm-1) and removal of the 3436.6-698.410 cm-1 band. The band at 1032.5-94.891 cm-1 indicated C-O stretching vibrations in cellulose and hemicelluloses.The presence of lignin was confirmed by aromatic skeletal vibrations (1718.3-96.397 cm-1 and 2118.4-99.531 cm-1). The band at 1375.4-84.363 cm-1 represented C-H deformation of the CH3 group in acetyl. The FTIR spectra demonstrated the removal of pectin and waxes from the bagasse filler surface, enhancing bonding and adhesion between the filler and low-density polyethylene matrix. Acetylation introduced ester groups in cellulose, as evident from the comparison between treated and non-treated PEC.

3.11 Dynamic Mechanical Analysis (DMA)

DMA is a technique that applies cyclic loading to a sample, permitting the material's response to stress, temperature, and frequency to be assessed. The analysis provides information on a specimen's mechanical properties as a function of time and temperature.

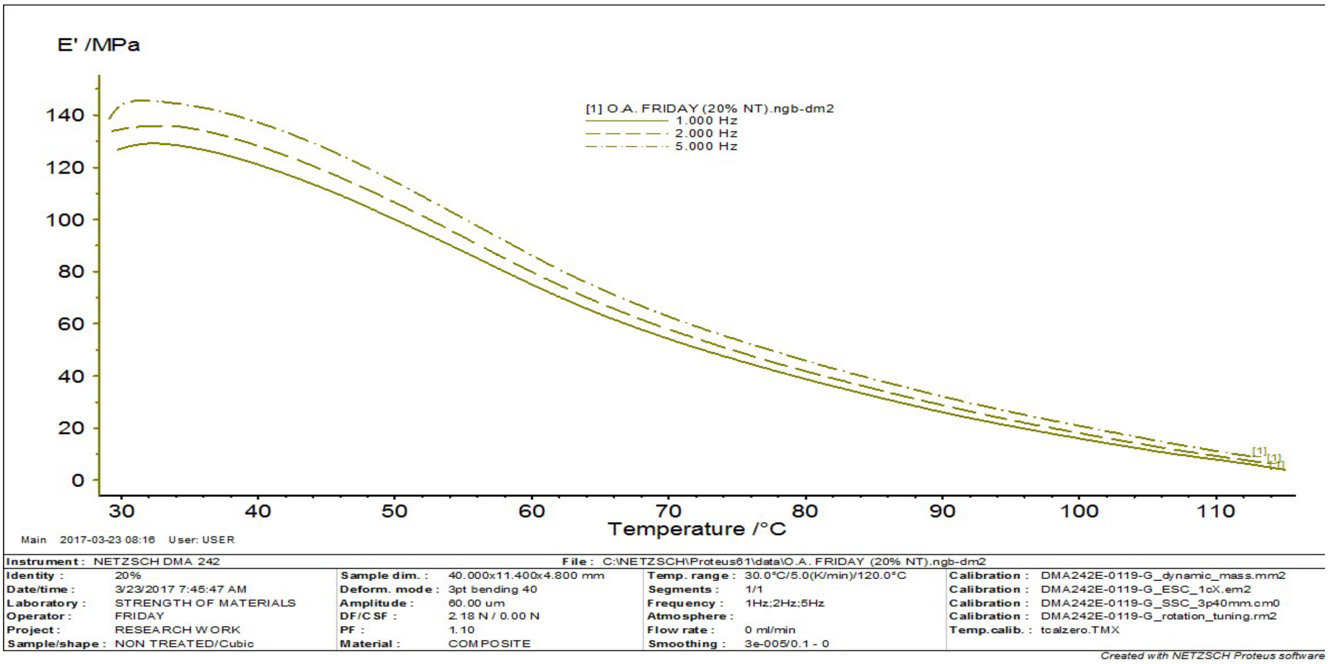

Instrument :	NETZSCH DMA 242			**File :**	C:\NETZSCH\Proteus61\data\O.A. FRIDAY (20% NT).ngb-dm2		
Identity :	20%	**Sample dim. :**	40.000x11.400x4.800 mm	**Temp. range :**	30.0°C/5.0(K/min)/120.0°C	**Calibration :**	DMA242E-0119-G_dynamic_mass.mm2
Date/time :	3/23/2017 7:45:47 AM	**Deform. mode :**	3pt bending 40	**Segments :**	1/1	**Calibration :**	DMA242E-0119-G_ESC_1cX.em2
Laboratory :	STRENGTH OF MATERIALS	**Amplitude :**	60.00 um	**Frequency :**	1Hz;2Hz;5Hz	**Calibration :**	DMA242E-0119-G_SSC_3p40mm.cm0
Operator :	FRIDAY	**DF/CSF :**	2.18 N / 0.00 N	**Atmosphere :**		**Calibration :**	DMA242E-0119-G_rotation_tuning.rm2
Project :	RESEARCH WORK	**PF :**	1.10	**Flow rate :**	0 ml/min	**Temp.calib. :**	tcalzero.TMX
Sample/shape :	NON TREATED/Cubic	**Material :**	COMPOSITE	**Smoothing :**	3e-005/0.1 - 0		

Created with NETZSCH Proteus software

Figure 14: The Variation of Storage Modulus' of non-treated bagasse filler LDPEC with temperature

Received: 15-03-2025 / Accepted: 19-05-2025 / Published: 29-09-2025
https://doi.org/10.70118/ujet.2025.0202.37

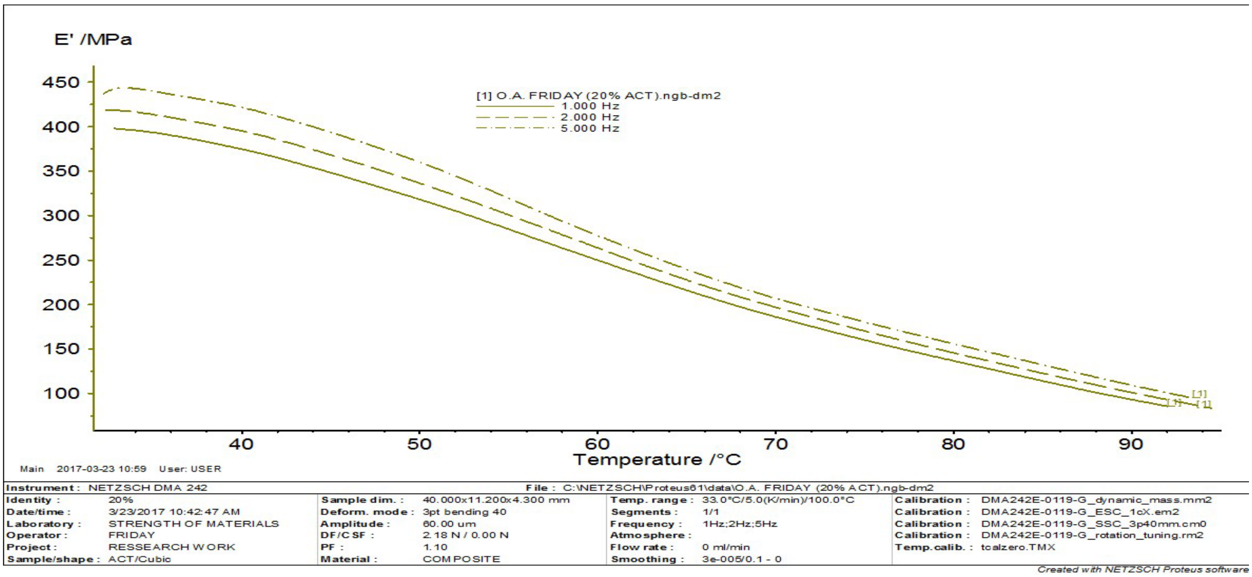

Instrument: NETZSCH DMA 242   File: C:\NETZSCH\Proteus61\data\O.A. FRIDAY (20% ACT).ngb-dm2

Identity :	20%	Sample dim. :	40.000x11.200x4.300 mm	Temp. range :	33.0°C/5.0(K/min)/100.0°C	Calibration :	DMA242E-0119-G_dynamic_mass.mm2
Date/time :	3/23/2017 10:42:47 AM	Deform. mode :	3pt bending 40	Segments :	1/1	Calibration :	DMA242E-0119-G_ESC_1cX.em2
Laboratory :	STRENGTH OF MATERIALS	Amplitude :	60.00 um	Frequency :	1Hz;2Hz;5Hz	Calibration :	DMA242E-0119-G_SSC_3p40mm.cm0
Operator :	FRIDAY	DF/CSF :	2.18 N / 0.00 N	Atmosphere :		Calibration :	DMA242E-0119-G_rotation_tuning.rm2
Project :	RESSEARCH WORK	PF :	1.10	Flow rate :	0 ml/min	Temp.calib. :	tcalzero.TMX
Sample/shape :	ACT/Cubic	Material :	COMPOSITE	Smoothing :	3e-005/0.1 - 0		

Figure 15: The Variation of Storage Modulus of acetylated treated bagasse filler LDPEC with temperature

3.12 Storage Modulus

The storage modulus (E') represents the stiffness of a viscoelastic material, proportional to the energy stored during loading cycles. It is the real part of the material's complex modulus.DMA analysis of 20%wt bagasse filler-reinforced LDPEC showed that storage modulus decreases with increasing temperature for both treated and non treated samples (Figures 14 and 15).

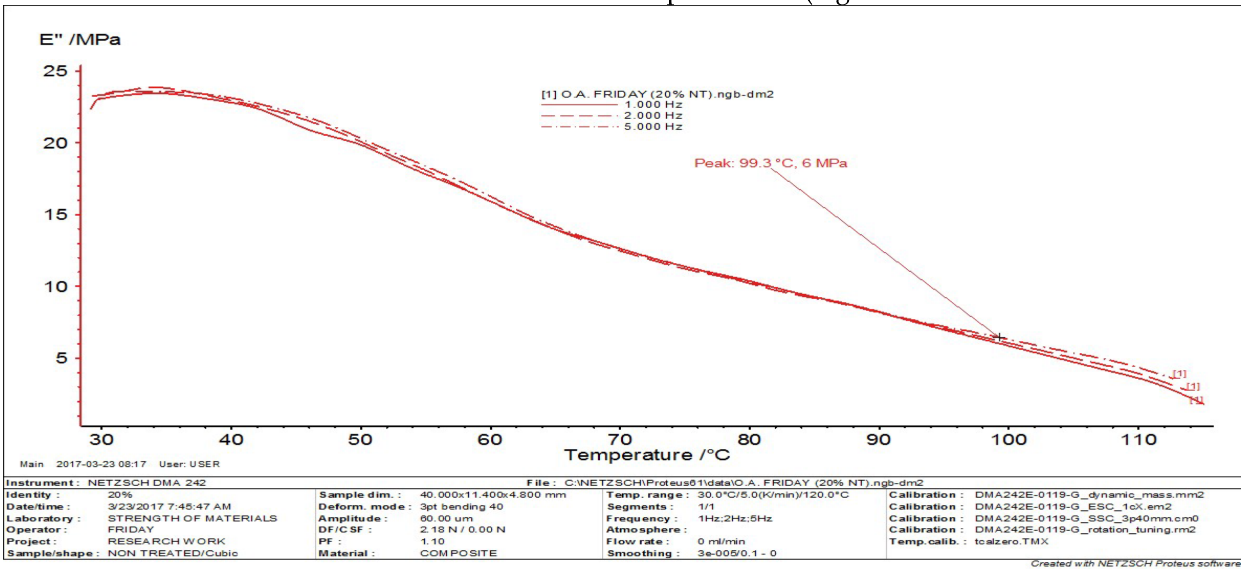

Instrument: NETZSCH DMA 242   File: C:\NETZSCH\Proteus61\data\O.A. FRIDAY (20% NT).ngb-dm2

Identity :	20%	Sample dim. :	40.000x11.400x4.800 mm	Temp. range :	30.0°C/5.0(K/min)/120.0°C	Calibration :	DMA242E-0119-G_dynamic_mass.mm2
Date/time :	3/23/2017 7:45:47 AM	Deform. mode :	3pt bending 40	Segments :	1/1	Calibration :	DMA242E-0119-G_ESC_1cX.em2
Laboratory :	STRENGTH OF MATERIALS	Amplitude :	60.00 um	Frequency :	1Hz;2Hz;5Hz	Calibration :	DMA242E-0119-G_SSC_3p40mm.cm0
Operator :	FRIDAY	DF/CSF :	2.18 N / 0.00 N	Atmosphere :		Calibration :	DMA242E-0119-G_rotation_tuning.rm2
Project :	RESEARCH WORK	PF :	1.10	Flow rate :	0 ml/min	Temp.calib. :	tcalzero.TMX
Sample/shape :	NON TREATED/Cubic	Material :	COMPOSITE	Smoothing :	3e-005/0.1 - 0		

Figure 16: The Variation of Loss Modulus of non treated bagasse filler LDPEC with temperature

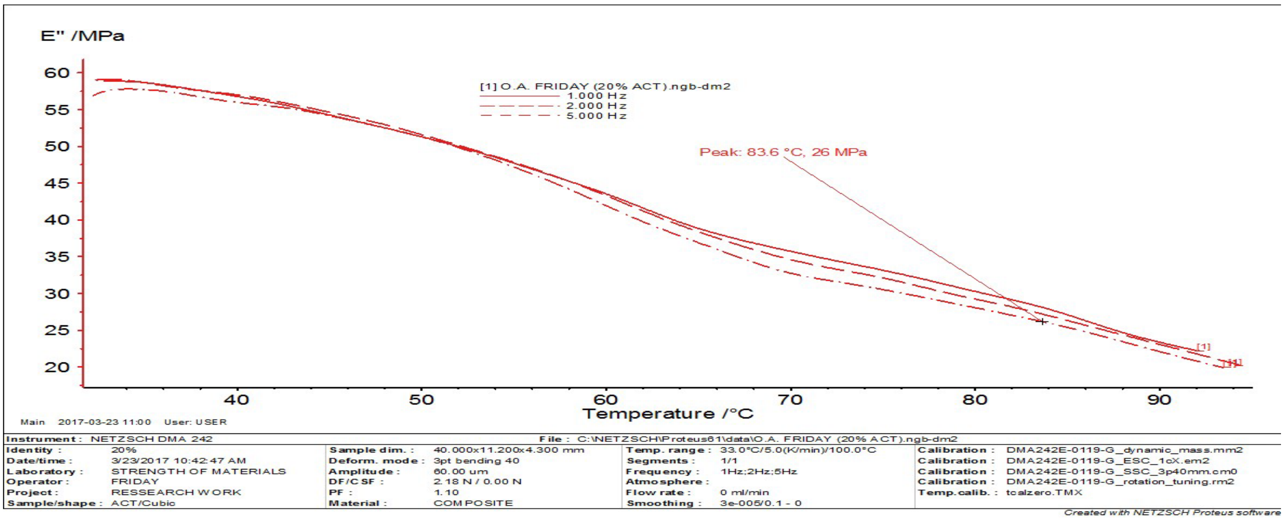

Instrument: NETZSCH DMA 242   File: C:\NETZSCH\Proteus61\data\O.A. FRIDAY (20% ACT).ngb-dm2

Identity :	20%	Sample dim. :	40.000x11.200x4.300 mm	Temp. range :	33.0°C/5.0(K/min)/100.0°C	Calibration :	DMA242E-0119-G_dynamic_mass.mm2
Date/time :	3/23/2017 10:42:47 AM	Deform. mode :	3pt bending 40	Segments :	1/1	Calibration :	DMA242E-0119-G_ESC_1cX.em2
Laboratory :	STRENGTH OF MATERIALS	Amplitude :	60.00 um	Frequency :	1Hz;2Hz;5Hz	Calibration :	DMA242E-0119-G_SSC_3p40mm.cm0
Operator :	FRIDAY	DF/CSF :	2.18 N / 0.00 N	Atmosphere :		Calibration :	DMA242E-0119-G_rotation_tuning.rm2
Project :	RESSEARCH WORK	PF :	1.10	Flow rate :	0 ml/min	Temp.calib. :	tcalzero.TMX
Sample/shape :	ACT/Cubic	Material :	COMPOSITE	Smoothing :	3e-005/0.1 - 0		

Figure 17: The Variation of Loss Modulus of acetylated treated bagasse filler LDPEC with temperature

https://doi.org/10.70118/ujet.2025.0202.37

The NTBF LDPEC's storage modulus decreased with temperature for all three frequencies applied (1 Hz, 2 Hz, and 5 Hz), with maximum values of 130 MPa, 135 MPa, and 140 MPa at 30°C (Figure 14).In contrast, the ACTBF LDPEC exhibited higher storage modulus values, attributed to improved interfacial bonding between the matrix and bagasse filler caused by chemical treatment (Figures 15). The ACTBF LDPEC's storage modulus reached a maximum value of 450 MPa at 30°C, confirming that chemical treatment enhances interfacial adhesion and the real part of the material's complex modulus.

3.13 Loss Modulus (E'')

The loss modulus decreased with increasing temperature for both bagasse filler LDPECs, as shown in Figures 16 and 17. The NTBF LDPEC exhibited the highest temperature peak at 99.3°C, followed by the ACTBF LDPEC at 83.3°C. The loss modulus peak values were 26 MPa for ACTBF LDPEC and 6 MPa for NTBF LDPEC, indicating that more energy is dissipated during the loading cycle for treated bagasse fillers compared to NTBF LDPEC (Julien et al., 2010).

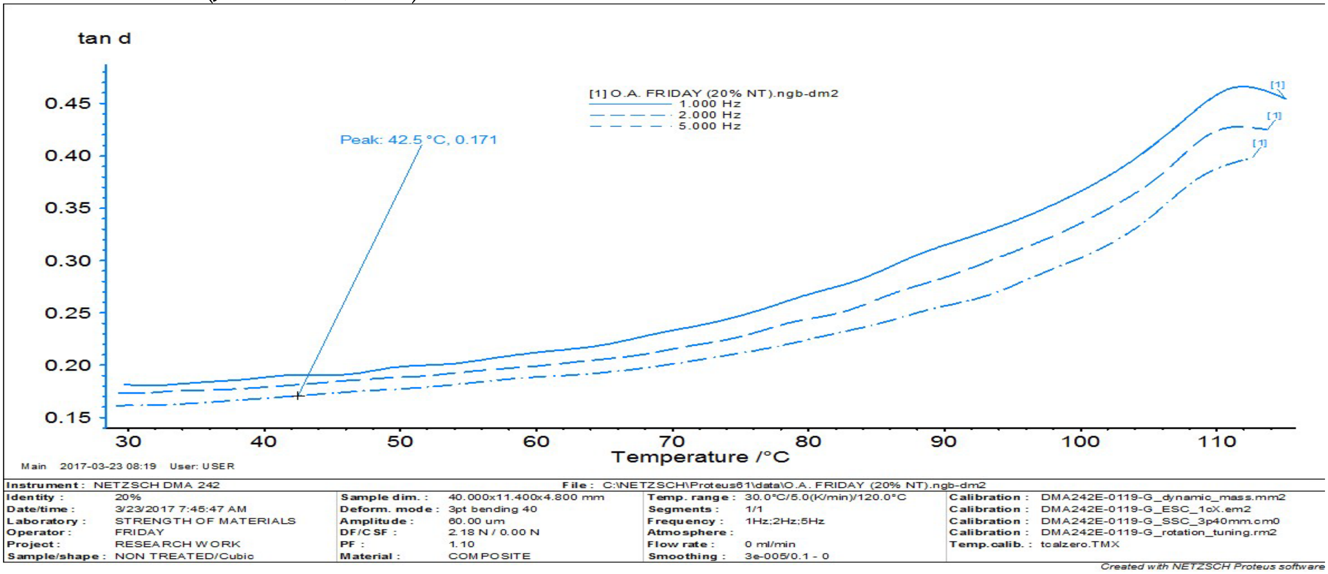

Instrument : NETZSCH DMA 242
File : C:\NETZSCH\Proteus61\data\O.A. FRIDAY (20% NT).ngb-dm2
Identity : 20%
Date/time : 3/23/2017 7:45:47 AM
Laboratory : STRENGTH OF MATERIALS
Operator : FRIDAY
Project : RESEARCH WORK
Sample/shape : NON TREATED/Cubic
Sample dim. : 40.000x11.400x4.800 mm
Deform. mode : 3pt bending 40
Amplitude : 60.00 um
DF/CSF : 2.18 N / 0.00 N
PF : 1.10
Material : COMPOSITE
Temp. range : 30.0°C/5.0(K/min)/120.0°C
Segments : 1/1
Frequency : 1Hz;2Hz;5Hz
Atmosphere :
Flow rate : 0 ml/min
Smoothing : 3e-005/0.1 - 0
Calibration : DMA242E-0119-G_dynamic_mass.mm2
Calibration : DMA242E-0119-G_ESC_1cX.em2
Calibration : DMA242E-0119-G_SSC_3p40mm.cm0
Calibration : DMA242E-0119-G_rotation_tuning.rm2
Temp.calib. : tcalzero.TMX

Figure 18: The Variation of Loss Factor of non-treated bagasse filler LDPEC with temperature

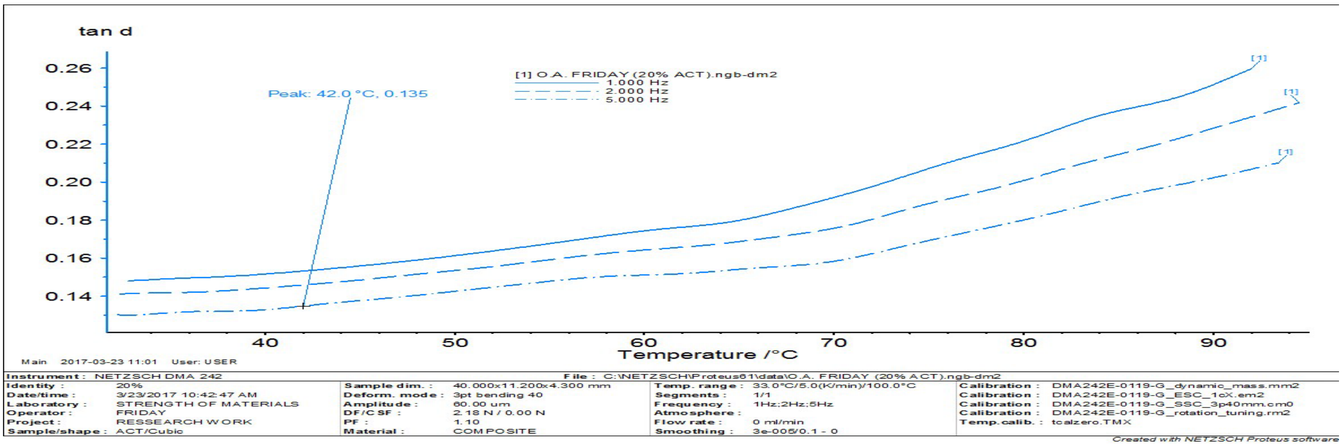

Instrument : NETZSCH DMA 242
File : C:\NETZSCH\Proteus61\data\O.A. FRIDAY (20% ACT).ngb-dm2
Identity : 20%
Date/time : 3/23/2017 10:42:47 AM
Laboratory : STRENGTH OF MATERIALS
Operator : FRIDAY
Project : RESSEARCH WORK
Sample/shape : ACT/Cubic
Sample dim. : 40.000x11.200x4.300 mm
Deform. mode : 3pt bending 40
Amplitude : 60.00 um
DF/CSF : 2.18 N / 0.00 N
PF : 1.10
Material : COMPOSITE
Temp. range : 33.0°C/5.0(K/min)/100.0°C
Segments : 1/1
Frequency : 1Hz;2Hz;5Hz
Atmosphere :
Flow rate : 0 ml/min
Smoothing : 3e-005/0.1 - 0
Calibration : DMA242E-0119-G_dynamic_mass.mm2
Calibration : DMA242E-0119-G_ESC_1cX.em2
Calibration : DMA242E-0119-G_SSC_3p40mm.cm0
Calibration : DMA242E-0119-G_rotation_tuning.rm2
Temp.calib. : tcalzero.TMX

Figure 19 : The Variation of Loss Factor of acetylated treated bagasse filler LDPEC with temperature

3.14 Loss Factor (Tan δ)

The loss factor increased with temperature for both LDPECs, as shown in Figures 18 and 19. The peak loss factor values were 0.171 at 42.5°C for NTBF LDPEC and 0.135 at 42.0°C for ACTBF LDPEC. The chemically treated bagasse filler PEC exhibited lower loss factor values, indicating more elastic properties compared to the non-treated bagasse filler LDPEC. In contrast, the NTBF LDPEC showed more non-elastic strain components.

4.0 Conclusion and Recommendation

4.1 Conclusion

This research investigated the effect of acetylation treatments on the properties of bagasse filler polyethylene composites. The following conclusions were drawn:

1. Chemical treatments improved the water absorption rate from 1% to 0.4% at 10wt% filler loading, 2.9% to 0.4 for 20% filler loading and 3% to 0.7% for 30% filler loading, young modulus 22.1Mpa to 25.3Mpa for 20% filler loading, impact strength 11- 14.3 for 10% filler loading, 10.3 to 13.3 for 20% filler loading and 10- 11.7J for 30% filler loading in the LDPEC and 12 to 14%, 14 to 17% and 18 to 29.3% for 10, 20 and 30% filler loading increase in percentage elongation of the polyethylene composite (LDPEC).
2. The tensile and flexural strength of untreated and treated bagasse filler LDPECs reached maximum values at 30% at 4.6 to 6.9Mpa for tensile strength and 40% at weight fractions, respectively.
3. The mechanical, morphological, and water absorption properties of chemically treated bagasse filler LDPECs were significantly different from those of untreated LDPECs.
4. Acetylation treatment was found to be the optimum effect for enhancing the mechanical properties and water absorption of LDPEC.

4.2 Recommendation

For optimal performance of bagasse filler polyethylene composites, it is recommended that: The filler be treated with a 5% acetylation solution and the filler loading be 30% weight fraction.

References

Agunsoye, J. O., & Aigbodion, V. S. (2013). Bagasse-filled recycled polyethylene bio-composites: Morphological and mechanical properties study. *Results in Physics*, 3, 187–194.

Beroti, A. R., Luporini, S., & Esperidião, M. C. (2009). Effects of acetylation in vapour phase and mercerisation on the properties of sugarcane fibres. *Carbohydrate Polymers*, 77, 20–24.

Bledzki, A. K., Mamun, A. A., & Volk, J. (2010). Barley husk and coconut shell reinforced polypropylene composites: The effect of fibre physical, chemical, and surface properties. *Composites Science and Technology*, 70(5), 840–846.

Campbell, F. C. (2021). *Structural Composite Materials*. ASM International

Chatterjee, S. (2021). *Reinforced Polymer Composites*: Process, Characterization and Applications. CRC Press

Dittenber, D. B., & Gangarao, H. V. S. (2012). Critical review of recent publications on the use of natural composites in infrastructure. *Composites Part A*: Applied Science and Manufacturing, 43, 1419–1429.

Gonzalez-Murillo, C., & Ansell, M. P. (2009). Mechanical properties of henequen fibre/epoxy resin composites. *Mechanics of Composite Materials*, 45, 435–442.

Gu, H. (2007). Tensile behaviours of coir fibre and related composites after sodium hydroxide treatment. *Materials & Design*, 30, 3931–3934.

Haque, M., Islam, S., Sakmul, S., Islam, N., Huque, H., & Hassan, M. (2010). Physico-mechanical properties of chemically treated palm fibre reinforced polypropylene composite. *Journal of Reinforced Plastics and Composites*, 29, 1734–1742.

Inuwa, I. (2013). Potential materials for food packaging from nanoclay/natural fibres filled hybrid composites. *Materials & Design*, 46, 391–410.

Jawaid, M., Thariq, M., & Saba, N. (Eds.). (2020). Mechanical and Physical Testing of Biocomposites, Fibre-
Reinforced Composites and Hybrid Composites. *Woodhead Publishing*.

Jiménez, A. M., López, J. A., & Vilaseca, F. (2020). Chemical modification of sugarcane bagasse fibers to improve compatibility with recycled high-density polyethylene. *Polymer Composites*, 41(4), 1192–1203. https://doi.org/10.1002/pc.22720

Liu, H., Zhang, Y., & Adekunle, K. (2023). Effect of chemical treatments on mechanical properties of sugarcane bagasse (Gramineae Saccharum officinarum L.) fiber-based biocomposites: A review

Mark, H. (2011). Defects in natural fibres: Their origin, characteristics, and implications for natural fibre-reinforced composites. Journal of Materials Science, 47, 599–609.

Miracle, D., & Donaldson, S. (2003). Introduction to composites. ASM Handbook, 21, 123–141.

Mohanty, A. K., Mishra, S., Drzal, L. T., Misra, M., Parija, S., & Nayak, S. K. (2003). Studies on the mechanical performance of biofibre/glass reinforced polyester hybrid composites. Composites Science and Technology, 63, 1337–1385.

Mulinari, D. R., Voorwald, H. J. C., Cioffi, M. O. H., Da Silva, M. L. C. P., & Lus, S. M. (2009). Preparation and properties of HDPE/sugarcane bagasse cellulose composite obtained using a thermo-kinetic mixer. Carbohydrate Polymers, 75(2), 317–321.

Munawar, S. S., Umemura, K., & Kawai, S. (2007). Characterisation of the morphological, physical, and mechanical properties of seven non-wood plant fibre bundles.. *Journal of Wood Science*, 53, 108–113.

Mwaikambo, L. Y., & Ansell, M. P. (2002). Chemical modification of hemp, sisal, jute, and kapok fibres by alkalisation. *Journal of Applied Polymer Science*, 84, 2222–2234.

Nair, L. S., & Laurencin, C. T. (2020). Biodegradable polymers as biomaterials. *Progress in Polymer Science*, 105, 101254

Nishino, T. (2004). Natural fibre sources, green composites: Polymer composites and the environment. In C. Baillie (Ed.), Green Composites: *Polymer Composites and the Environment* (pp. 49–65). Woodhead Publishing Ltd.

Oladele, I. O., Akinwekomi, A. D., & Akinlabi, S. A. (2020). Comparative evaluation of acetylation treatment on the constituents and properties of selected natural fibers. Fibers, 8(12), 73. https://doi.org/10.3390/fib8120073

Rahman, M.M., Hasan, M., and Chowdhury, M.A (2022): Improvement of mechanical properties of LDPE composites using treated sugar cane bagasse fiber. *Journal of Applied polymer science*, 139 (6)

Sain, M., Suhara, P., Law, S., & Bouilloux, A. (2005). Interface modification and mechanical properties of natural fibre-polyolefin composite products. *Journal of Reinforced Plastics and Composites*, 24, 121–129.

Silviana, S., Surjandari, I., & Dewi, D. (2018). Acetylation of cassava bagasse starch and microfibrillated cellulose from bamboo. *In Proceedings of the 3rd International Conference on Research, Implementation and Education of Mathematics and Science* (ICRIEMS) (Vol. 204, Article 01019). MATEC Web of Conferences. https://doi.org/10.1051/matecconf/201820401019

Satyanarayana, K. G., Arizaga, G. G. C., & Wypych, F. (2009). Biodegradable composites based on lignocellulosic fibres—An overview. *Journal of Polymer Science*, 34, 982–1021.

Sapieha, S., Allard, P., & Zang, Y. H. (2005). Dicumyl-peroxide-modified interface of Agave americana waste HDPE composites as possible roof ceilings in Lesotho. *Composite Interfaces*, 14, 821–836.

Tserki, V., Zafeiropoulos, N. E., Simon, F., & Panayiotou, C. (2005). A study of the effect of acetylation and propionylation surface treatments on natural fibres. *Composites Part A*: Applied Science and Manufacturing, 36(8), 1110–1118.

Valadez, G. A., Cervantes, J. M., Olayo, R., & Herrera-Franco, P. J. (1999). Effects of fibre surface treatment on fibre-matrix bond strength of natural fibre reinforced composites. *Composites Part B*: Engineering, 30(3), 309–320.

Zampaloni, M., Pourboghrat, F., Yankovich, S. A., Rodgers, B. N., Moore, J., Zrzal, L. T., Mohanty, A. K., & Misra, M. (2007). Kenaf natural fibre–reinforced polypropylene composite. *Composites Part A*: Applied Science and Manufacturing, 38(6), 1569–1580.

Zhang.Y., Li Y., and Wang, X. (2020): Influence of surface –treated natural Fibres on Mechanical and thermal properties of polyethylene composite. *Composite Part B*: Engineering, 191, 107939.

Received: 15-03-2025 / Accepted: 19-05-2025 / Published: 29-09-2025

https://doi.org/10.70118/ujet.2025.0202.37